RESEARCH ARTICLE

Tiagabine Incorporated Polymeric Microneedles: Formulation and Characterization Studies

Kadir Aykaç[1,2,3] and Ebru Başaran[1,*]

[1]*Department of Pharmaceutical Technology, Faculty of Pharmacy, Anadolu University, 26470 Tepebaşı, Eskişehir, Türkiye;* [2]*Department of Pharmaceutical Technology, Faculty of Pharmacy, Erzincan Binali Yıldırım University, 24002, Yalnızbağ, Erzincan, Türkiye;* [3]*Graduate School of Health Sciences, Anadolu University, 26470 Tepebaşı, Eskişehir, Türkiye*

© 2023 The Author(s). Published by Bentham Science Publisher. This is an open access article published under CC BY 4.0 https://creativecommons.org/licenses/by/4.0/legalcode

ARTICLE HISTORY

Received: March 01, 2023
Revision: March 27, 2023
Accepted: April 03, 2023

DOI:
10.2174/2452271606666230427091330

Abstract: ***Background*:** The oral route is the primary route for both acute and chronic treatment of epilepsy. However, lack of oral access during the seizures and high drug resistance limit the anti-epileptogenic effects of most antiepileptic drugs. Therefore, alternative routes and novel drug delivery systems are required. In this study, polymeric microneedles were formulated and characterized for possible intranasal administration of Tiagabine (TIA) in order to overcome the blood-brain barrier (BBB).

***Methods*:** In our study, carboxymethyl cellulose (CMC) and Eudragit® S 100 (ES100) based polymeric microneedles were formulated by micromolding method. Scanning electron microscopy (SEM), differential scanning calorimetry (DSC), X-ray diffractometry (XRD), fourier transform infrared spectroscopy (FT-IR) and proton nuclear magnetic resonance (^{1}H-NMR), *in vitro* release, and texture analyses were performed. For the stability analyses, formulations were kept at 25°C ± 2°C (60 ± 5% Relative Humidity; RH), 40°C ± 2°C (75 ± 5% RH) and 5°C ± 3°C for six months.

***Results*:** Analysis results revealed that robust microneedles were formulated successfully by micromolding method with adjustable needle lengths. Depending on the polymer type, sustained TIA releases up to 72 hours were achieved. Structural integrities were maintained at all storage conditions during the storage period of six months.

***Conclusion*:** TIA-loaded microneedles have the potential with less invasive properties, even with small amounts of TIA, through the unconventional nasal route for effective treatment of epilepsy.

Keywords: Tiagabine, epilepsy, microneedle, polymeric drug delivery systems, micromolding method, texture analysis, characterization studies.

1. INTRODUCTION

Epilepsy is a chronic neurological disorder with considerably high incidence regardless of age and requires long-term treatment [1]. Recurrent seizures and accompanying behavioral changes have a significant impact on the patients' daily life quality [2]. Antiepileptic drugs mainly control the incidence of seizures; however, 20-25% of the patients do not respond to antiepileptic therapy due to drug-resistant or refractory epilepsy [3]. Sudden unexplained death risks of 1-9 in 1000 cases require more sufficient treatments with novel drugs and drug delivery systems [4]. The blood-brain barrier (BBB) remains a significant obstacle to the efficient treatment of central nervous system disorders, including drug-resistant epilepsies [5]. Tight junctions of endothelial cells that separate the brain from the circulatory system protect the brain against harmful substances. Therefore, it is challenging to overcome the permeability barrier of BBB with conventional drug delivery systems [6, 7]. In recent years, intranasal drug delivery has gained more attention due to the high permeability of nasal epithelium, which provides a large absorption site for the rapid absorption of small and lipophilic molecules [8]. With a direct connection to the central nervous system, the nasal mucosa and the olfactory region pathway, the intranasal application provides a simple and non-invasive gateway to the brain with reduced systemic exposure minimizing the systemic adverse effects [6, 9]. The alteration of first-pass metabolism and low enzymatic activity also enhances most drugs' bioavailability with intranasal application [10]. Nasal epithelium acts as a barrier for hydrophilic drugs, and a rapid mucociliary clearance mechanism reduces the permeability of most applied drugs [11]. To overcome these limitations, different drug delivery systems like liposomes [5], aerosols [12], nanoparticles [13], nanostructured lipid carriers [8], powders [14], hydrogels [11] and inserts were formulated [15]. Microneedles are patch-like drug delivery systems with micron-sized needles coated or loaded with

*Address correspondence to this author at the Department of Pharmaceutical Technology, Faculty of Pharmacy, Anadolu University, 26470 Tepebaşı, Eskişehir, Türkiye; Tel: +90 533 7127422; E-mail: ebcengiz@anadolu.edu.tr

active agents [16]. Microneedles can be classified as solid, porous, hollow, coated, and biodegradable microneedles with heights ranging from 25 to 2000 μm with different needle shapes [17]. Various materials like silicone, stainless steel, titanium, and biodegradable or non-biodegradable polymers can fabricate the microneedles, affectinghe release characteristics and therapeutic performances of the microneedles [18, 19]. Microneedles overcome the biological barriers with physical penetration with less invasive way that makes them preferential for sufficient treatment [20]. Microneedles mostly formulated to overcome the barrier effect of the skin with their structural integrities [16]. The structure, geometry, formulation components, cross-linking density, degradation profiles, swelling properties, and responses to biological/physical stimuli influence the release rate of the drugs from microneedle patches [21]. Depending on the height, shape, and density of the needles, penetration through the stratum corneum to epidermis, and superficial dermis is possible for both local and systemic drug delivery [22]. However, recent studies showed that tailor-made microneedles can also be used for non-transdermal applications, such as those involving the eyes, blood vessels, or gastrointestinal tract [23, 24].

Tiagabine hydrochloride (TIA) ($C_{20}H_{26}ClNO_2S_2$) is a water-soluble anti-convulsive agent sold under the brand name of Gabitril® also used to treat panic disorders. It is a selective γ-aminobutyric acid (GABA) reuptake inhibitor used for patients aged 12 years and above [25, 26]. TIA is readily absorbed after oral administration and is widely distributed through the body, with maximum plasma concentrations within two hours [27]. The presence of nipecotic acid coupled to a lipophilic side-chain facilitates penetration of TIA through the blood-brain barrier (BBB). It inhibits GABA uptake into both neurons and glia, which explains the efficacy of the active agent [26, 28]. However, treatment with TIA may cause side effects such as drowsiness, dizziness, lack of concentration, and vision problems with poor coordination [29]. In our study, TIA-incorporated polymeric microneedles were formulated with carboxymethyl cellulose (CMC) and Eudragit® S 100 (ES100) aiming nasal application to overcome the BBB for enhanced therapeutic effect with minimizing the side effects with reduced applied doses. Morphological and structural analyses were performed to evaluate the potential of TIA-incorporated polymeric microneedles for nasal delivery and subsequent *in vivo* studies.

2. EXPERIMENTAL

2.1. Materials

Tiagabine was purchased from Toronto Research Chemicals (Ontario, Canada). Acetonitrile, deuterium oxide, deutero-chloroform, deutero-dimethyl sulfoxide, methanol, polyethylene glycol 400 were the products of Merck (Darmstadt, Germany). Eudragit® S 100 was from Röhm Pharma (Darmstadt, Germany), glycerine was from Riedel-de Haën (Seelze, Germany). Hydroxypropyl-γ-cyclodextrin and carboxymethyl cellulose were from Sigma (Steinheim, Germany), and polysiloxane was from Zhermack SPA (Rovigo, Italy). All other chemicals used were of analytical grade.

2.2. Methods

2.2.1. Analytical Method Validation

A modified high-performance liquid chromatography (HPLC) method was used to determine TIA [30]. Analyses were performed using a Shimadzu 20-A (Japan) HPLC system (automatic injection with PDA detector) with a C18 column (diameter: 4.6 mm, length: 25.0 cm, particle diameter: 5 μm, and particle size: 100 Å) at 254 nm and 40ºC column temperature. Analyses were carried out using a mixture of Acetonitrile: Methanol: Distilled Water (37 : 10 : 53; *v/v*) as the mobile phase, with a flow rate of 1 $mL.min^{-1}$. Analytical method validation studies were performed according to ICH guidelines [31].

2.2.2. Microneedle Preparation

Microneedles were prepared by the micromolding method using CMC and ES100 to form water-soluble (dissolving) and water-insoluble polymeric microneedles, respectively [32]. In this method, microneedle molds were prepared using polysiloxane dental casting mixture (PDM) (polysiloxane: activator, [10: 1]; w/w) and Dermapen® titanium solid needles were used as master needle structures. After the preparation of PDM molds, Dermapen® needles were inserted into the molds and kept in touch for 30 minutes at 25°C ± 2°C for the formation of needle gaps, and then, the titanium needles were removed, and negative molds were obtained. The depth of the needle gaps was adjustable for forming polymeric needles with variable needle heights. Polymeric dispersions with different compositions were prepared. Dispersions were then poured into the molds and were settled by centrifugation (7500 rpm for 4 x10 min). After the centrifugation step, molds were kept at 50°C ± 1°C for the evaporation of the solvent for up to 24 hours. At the end of the drying period, the microneedles were removed from the molds and stored in tightly closed containers until analyzed [22, 32].

2.2.3. Characterization of Microneedles

2.2.3.1. Morphological Analyses

Scanning electron microscopy (SEM) was used to investigate the morphology of the prepared microneedles. The analysis was carried out using a Carl Zeiss SUPRA 50VP SEM (Oberkochen, Germany) at a room temperature of 25°C ± 2°C and a voltage of 3 kV with different magnifications. Photomicrographs were taken to assess the morphology of the microneedles visually.

2.2.3.2. Thermal Analyses

Differential scanning calorimetry (DSC) was used to analyze the thermal behaviors of the microneedles using DSC-60 (Shimadzu, Tokyo, Japan) instrument within the range of 30°C - 300°C at a heat flow rate of $10°C.min^{-1}$. Analyses were performed under a nitrogen atmosphere with a flow rate of 50 $mL.min^{-1}$. An empty aluminum cell was used as a reference for the analyses. DSC thermograms of pure materials were used as references for the comparison of the possibility of crystallinity changes in the structures

2.2.3.3. X-ray Diffractometry Analyses

X-ray diffraction (XRD) spectra of pure TIA, polymers, physical mixtures and microneedle samples were recorded

using MiniFlex 600 (Rigaku Corporation, Tokyo, Japan) under CuKα radiation at 30 kV of voltage and 40 mA with a scanning rate of 2θ/min over 2 diffraction angle within the range of 5°-70°. XRD diffractograms of pure polymers, physical mixtures and pure TIA were used as references for evaluating the crystallinity changes of the materials throughout the formulation stages.

2.2.3.4. Fourier Transform Iınfrared Analyses

Fourier transform infrared spectroscopy (FT-IR) analyses were carried out using deuterated triglycinesulfate doped with L-alanine detector used with Germanium-coated KBr plate beam splitter within the range of 400 cm^{-1} and 4000 cm^{-1} using Shimadzu IR Prestige-21 (Tokyo, Japan). FT-IR spectra of pure polymers and pure TIA were used as references for the determination of structural changes during formulation stages and stability conditions.

2.2.3.5. Nuclear Magnetic Resonance Analyses

Proton nuclear magnetic resonance (^{1}H-NMR) analyses were performed using Bruker 300 (Bruker Bioscience, Billerica, MA, USA). Samples were prepared by dissolving formulations in deutero-chloroform ($CDCI_3$) and deuterium oxide (D_2O). ^{1}H-NMR spectra of pure polymers and pure TIA were used as references for the determination of structural changes during formulation stages and stability conditions.

2.2.3.6. Texture Analyses

The mechanical properties of the microneedles were determined using Texture Analyzer (TA.XT plus, Stable Micro Systems, England). Microneedle patches were attached gently to the probe in a vertical position. Parafilm® M was used as a membrane alternative for this study. Parafilm was folded in eight layers to achieve a thickness of about 1 mm and fixed to the 30 mm base plate for uniform adhesion. The microneedles were attached to the cylindrical plate using double-sided tape with the needles facing down to determine the penetration force and puncture depths. The texture analyzer was set to compression mode and with a trigger force up to 42 N to the parafilm surface, with a speed of 0.1 mm. s^{-1} and the microneedles were observed to progress through the parafilm by stabilizing the pressure for 15 seconds (n = 3). Parafilm samples obtained were also examined with a stereomicroscope (Leica M205C, Germany) for the determination of puncture depths [24, 33].

2.2.4. Determination of Tiagabine

TIA amounts of the microneedles were evaluated by HPLC analyses. Briefly, accurately weighed (10 mg) microneedle samples were completely dissolved in water or methanol for CMC and ES100-based microneedles, respectively. HPLC analyses were performed after proper dilutions (n = 3).

2.2.5. In vitro Drug Release and Release Kinetics

In vitro release behaviour of TIA from polymeric microneedles was evaluated in phosphate buffer solution (37°C ± 1°C, 35mL, pH: 6.4) for 72 hours [10]. In the *in vitro* release studies, microneedles were attached to magnets with insoluble adhesives and kept attached to the sidewall of the flask to ensure active substance release from only the surfaces of the microneedles under constant mixing of the release medium at 250 rpm [20]. Samples were collected for 72 hours, and the equal amounts with the samples of fresh medium were added to the dissolution medium to maintain sink conditions. TIA amounts were evaluated by HPLC analyses after proper dilutions (n = 3). Analysis results were also assessed by DDSolver Program for the determination of release characteristics of TIA from polymeric microneedles [34].

2.2.6. Stability Studies

Formulations were stored in three different conditions: 25°C ± 2°C (60 ± 5% Relative Humidity; RH), 40°C ± 2°C (75 ± 5% RH) and 5°C ± 3°C for six months for stability studies. Changes in TIA amounts were determined and DSC, FT-IR and ^{1}H-NMR analyses were performed for the determination of structural changes.

3. RESULTS AND DISCUSSION

3.1. Analytical Method Validation

A modified HPLC method was used for the determination of TIA [30]. Analytical method validation was performed according to the ICH guidelines [31]. In linearity studies, R^2 was 0.9999 (y = 38130x - 10044) while accuracy was within the range of 99.0%-102.6%. RSD values were below 2% in precision studies. The selectivity of the method was analyzed with the comparison of HPLC signals of TIA against placebo formulations [31]. The stability of TIA in the mobile phase and the dissolution medium was also determined and was found stable during the analysis periods.

3.2. Microneedle Preparation

Micromolding method was used to formulate polymeric microneedles [32]. Many formulations with different polymers with different compositions and concentrations were formulated in preliminary studies. Considering fragility, physical integrity, and flexibility, CMC and ES100-based formulations were selected for further studies (Table **1**).

3.3. Characterization of Microneedles

3.3.1. Morphological Analyses

Needle sizes can be optimized considering the application routes by the micromolding method. Compositions of the dispersions and incorporation of TIA into the microneedles have an impact on the shapes of the needle tops [35]. SEM analyses revealed that CMC microneedles have more sharpened spear-like needle tops with an average height of 0.97 ± 0.02 mm while ES100 microneedles have rather blunt tops with uniform structures with an average height of 0.53 ± 0.01 mm (Fig. **1**). The analysis results indicated that the incorporation of TIA had a remarkable effect on the needle structures, especially for ES100-based microneedles. The addition of TIA to the ES100 solution affected the viscosity of the solution, resulting in uneven and insufficient settlement during the centrifugation step, which led to the formation of shorter needles with rather blunt tops (Fig. **1**).

3.3.2. Thermal Analyses

Polymeric structures undergo thermal changes that can affect their mechanical properties and degradation rates,

Table 1. Compositions of the selected formulations.

Code	TIA (mg)	CMC (mg)	HPGCD* (mg)	ES100 (mg)	PEG 400 (µL)	Methanol (mL)	Distilled Water (mL)
C0	-	60	20	-	-	-	1
C1	5	60	20	-	-	-	1
C2	10	60	20	-	-	-	1
E0	-	-	-	75	5	1	-
E1	5	-	-	75	5	1	-
E2	10	-	-	75	5	1	-

Note: *Hydroxypropyl-γ-cyclodextrin.

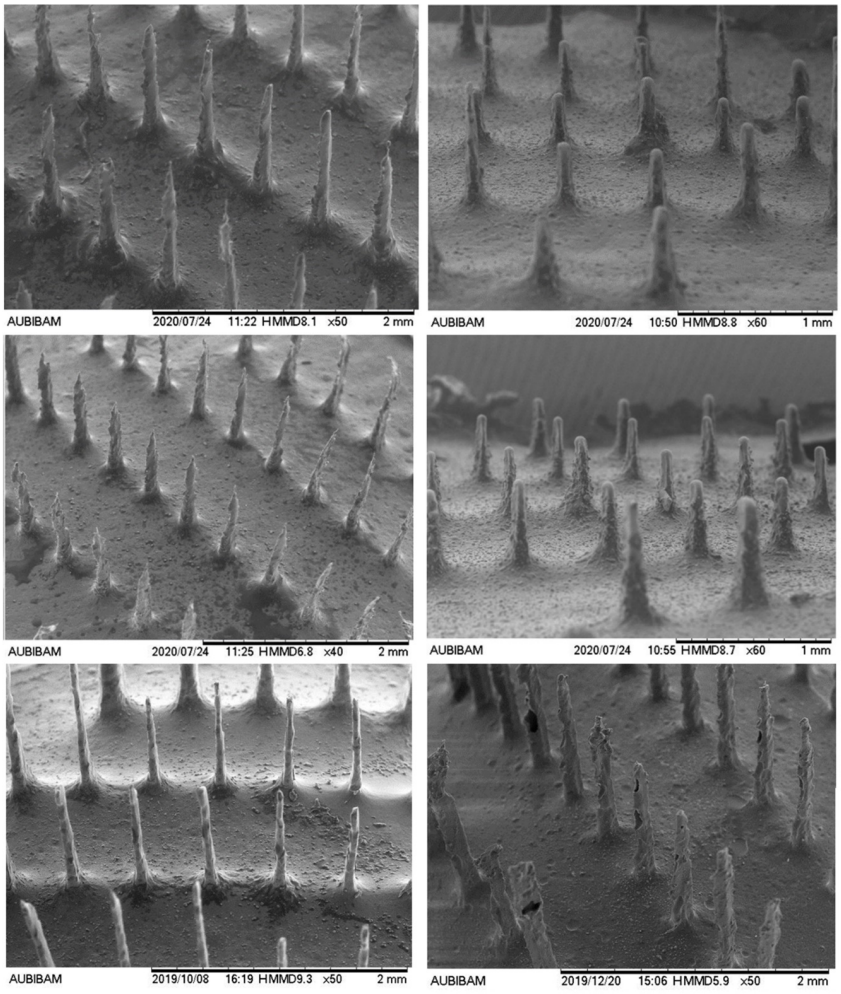


Fig. (1). SEM micro images of the microneedles (Left column CMC-based microneedles: C0, C1, and C2 (bottom to top) and right column ES100-based microneedles: E0, E1, and E2 (bottom to top)). *(A higher resolution / colour version of this figure is available in the electronic copy of the article).*

ultimately impacting the drug release rates of polymeric drug delivery systems. For this reason, DSC analyses were conducted to determine the thermal behaviors of the microneedles [36, 37]. An endothermic melting peak at 198.6 °C was recorded for TIA. Melting peaks were also revealed in physical mixture samples indicating the absence of any chemical interactions between the formulation components (as marked with arrows) (Fig. **2**). No endothermic signals were detected in the thermograms of the pure polymers showing their amorphous structures. As stated previously by Sanandiya

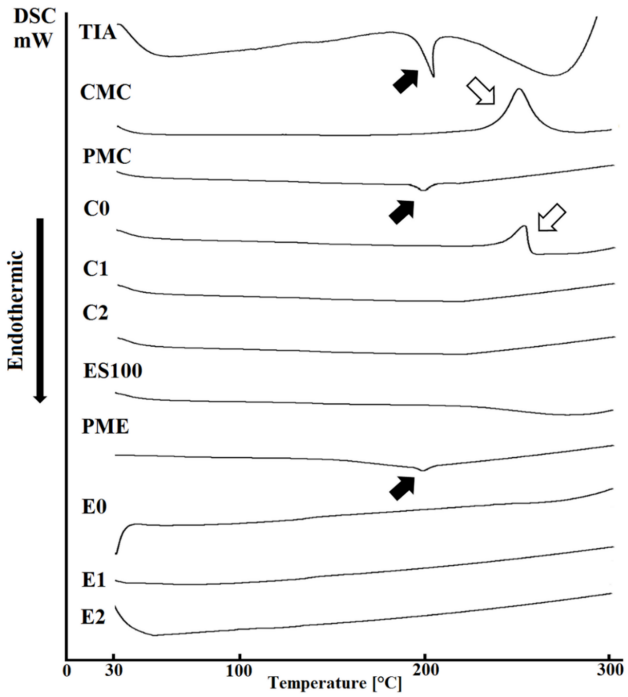


Fig. (2). DSC thermograms of the pure materials, physical mixtures, and the microneedles (PMC: Physical mixture of the CMC formulations excipients, PME: Physical mixture of the ES100 formulations excipients, endothermic melting peaks of TIA was marked with arrows). *(A higher resolution / colour version of this figure is available in the electronic copy of the article).*

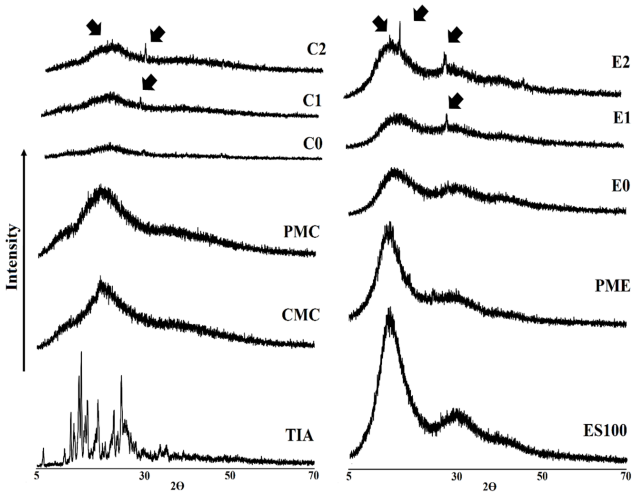


Fig. (3). XRD spectra of the pure materials, physical mixtures, and the microneedles (PMC: Physical mixture of the CMC formulations excipients, PME: Physical mixture of the ES100 formulations excipients). *(A higher resolution / colour version of this figure is available in the electronic copy of the article).*

and Siddhanta (2016); CMC and C0 showed exothermic peaks around 250°C due to the mass loss at elevated temperatures (as marked with hollow arrows); however, the C1 and C2 formulations did not show any similar peaks, indicating that the incorporation of TIA has influenced the physical integrity of the polymeric structure (Fig. **2**) [38]. No signals were recorded for C1, C2, and ES100-based microneedles showing the amorphous forms. The disappearance of the endothermic melting peaks of the TIA in the microneedles corresponds to the fact that it is no longer in a crystalline state in the formulations.

3.3.3. X-ray Diffractometry Analyses

The XRD spectra of pure TIA, polymers, and physical mixtures were used as references to determine the changes in crystallinity during microneedle formation. Analysis results showed that TIA was in a crystalline form and the polymers were in an amorphous form prior to the formulation stages (Fig. **3**) [39, 40]. For physical mixtures, the intensity of the signals changed slightly, especially within the range of 5-30 Θ. Still, the crystallinity of TIA could not be determined, as was revealed in the DSC analyses. However, after the formation of microneedles, despite the small changes in intensity

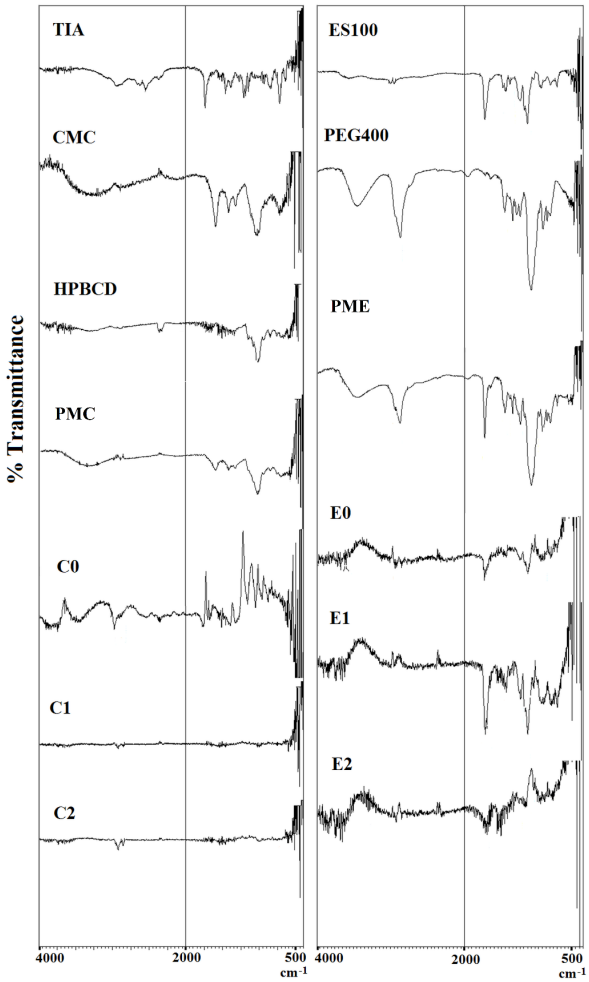


Fig. (4). FT-IR spectra of the pure materials, physical mixtures, and the microneedles (PMC: Physical mixture of the CMC formulations excipients, PME: Physical mixture of the ES100 formulations excipients). *(A higher resolution / colour version of this figure is available in the electronic copy of the article).*

in accordance with the increased amount of TIA (marked with arrows), the formulations showed amorphous structures in accordance with DSC analyses (Fig. **3**) [39]. Previous studies by several research groups, such as Sanandiya and Siddhanta (2016) and El-Sakhawy (2017), clearly revealed the amorphous structure of CMC by XRD analyses [38, 40]. The nanoparticles were formulated with ES100 by the Thakral *et al*. (2010) research group, and XRD analyses stated the amorphous structure of the polymer in accordance with our studies. Even after the crystalline drug's incorporation, the microparticles' diffractograms were also in an amorphous form due to the dilution effect by the amorphous polymers, resulting in the molecular distribution of the active agent within the polymeric structure [40].

3.3.4. Fourier Transform Infrared Analyses

Structural changes during and after microneedle formations were determined by FT-IR analyses within the range of 400 cm^{-1} and 4000 cm^{-1} [41]. TIA showed characteristic signals for aromatic stretching for sulfur -S-C at 640 cm^{-1}, C-C vibrations at 1209 cm^{-1}, R-CH_3 at 1456 cm^{-1}, a strong C = O stretching band at 1734 cm^{-1} and -OH stretching band at 2900 cm^{-1} [42]. For CMC, asymmetric and symmetric stretching vibrations of -COO, and -OH stretching vibration were revealed in the spectrum at 1591 cm^{-1}, 1417 cm^{-1}, and 3493 cm^{-1}, respectively [39]. And for ES100; signals at 1450 cm^{-1} for -CH3 bending, at 1728 cm^{-1} for C = O, and at 2953 cm^{-1} due to the presence of O-H were revealed [43]. Most of the TIA signals were hindered by the excipients' signals due to the small amount of TIA in the microneedles. However, the influence of the incorporation of TIA could be determined by comparing the spectra of the formulations with placebo microneedles. Although the intensities of the characteristic signals were changed, no additional signals could be detected, indicating that no chemical bonds were formed during the formulation stages (Fig. **4**).

3.3.5. Nuclear Magnetic Resonance Analyses

^{1}H-NMR analyses were also performed to better determine possible chemical interactions and changes during the formulation and stability stages of the microneedles [37, 41]. Analysis results of pure materials and physical mixtures were used as references for the determination of structural changes. TIA signals were detected in both spectra of physical mixtures and microneedles at 1.5-2 ppm and 7 ppm and at 4 ppm and 7 ppm for CMC and ES100-based microneedles

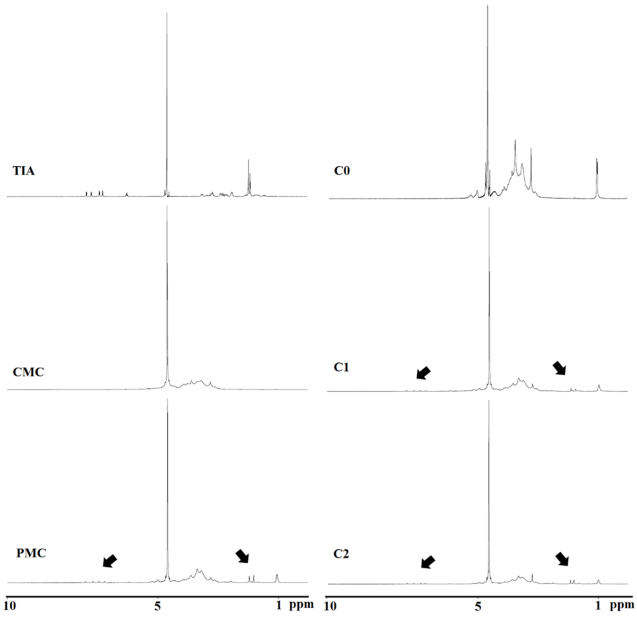


Fig. (5). [1]H-NMR spectra of the pure materials, physical mixtures, and the CMC-based microneedles (PMC: Physical mixture of the CMC formulations excipients, TIA signals marked with arrows). *(A higher resolution / colour version of this figure is available in the electronic copy of the article).*

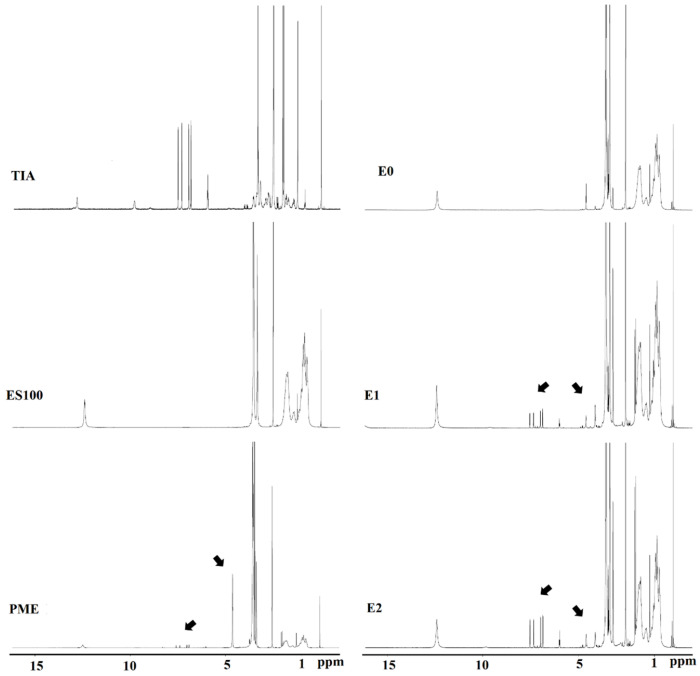


Fig. (6). [1]H-NMR spectra of the pure materials, physical mixtures, and the ES100-based microneedles (PME: Physical mixture of the ES100 formulations excipients, TIA signals marked with arrows). *(A higher resolution / colour version of this figure is available in the electronic copy of the article).*

(marked with arrows), respectively, showing that no chemical interactions were found between TIA and the formulation excipients (Figs. **5** and **6**) [42].

3.3.6. Texture Analyses

Tip diameter, needle geometry, and material composition all affect the strength of microneedles. Maintaining mechanical strength is a key issue for polymer-based microneedlesince they need to pierce membranes at the application sites [44]. In our study mechanical properties of the microneedles were determined using a Texture Analyzer [33]. The analysis results revealed that CMC-based microneedles could pass through 250 ± 25 μm with only 5N of force, while ES100-based formulations required higher application forces (Fig. **7**). The nasal epithelial cells have cilia on their surfaces which are responsible for mucociliary clearance, and each cell can have 200-300 cilia that are 5 to 10 μm in length. These cilia are covered by a layer of mucus that is 10-15 μm

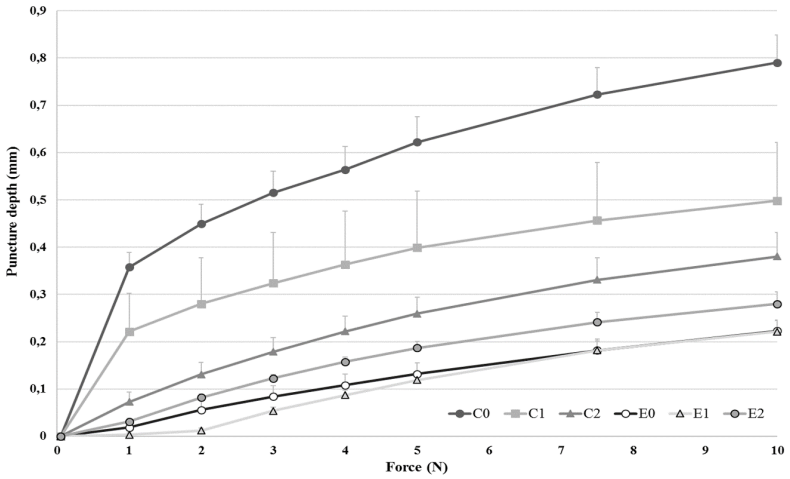


Fig. (7). Puncture depths of the microneedles under different puncture forces (Mean ± SE; n = 3).

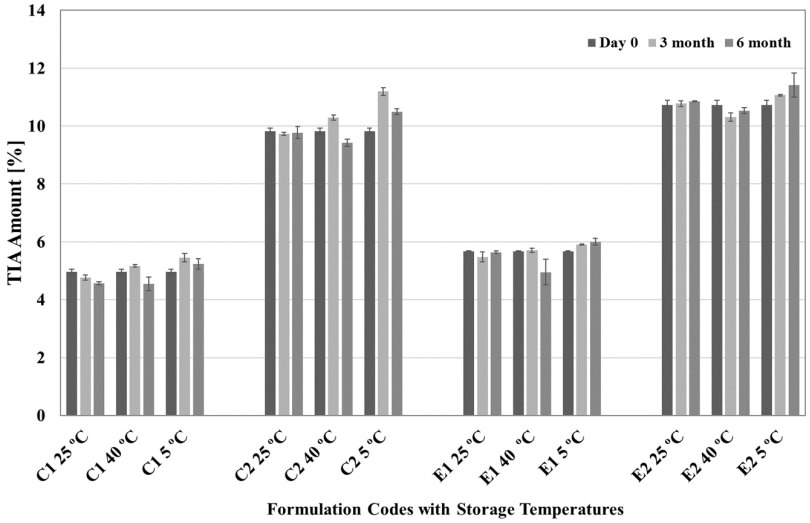


Fig. (8). TIA amounts at the day of production and during the storage period of six months (Mean ± SE; n = 3). *(A higher resolution / colour version of this figure is available in the electronic copy of the article).*

thick, and the spaces between the cilia are also filled with mucus [45]. Furthermore, the high amount of mucus secretion (1.5 - 2 L per day) and mucus turnover can limit the effectiveness of applied formulations. However, with the microneedle patches that we formulated, which have adjustable needle heights (0.97 ± 0.02 mm and 0.53 ± 0.01 mm for CMC and ES100-based microneedles, respectively), the barrier effect of the mucus layer can easily be overcome, resulting in longer residence durations for enhanced therapeutic effects, even with small amounts of TIA. Microneedles offer a promising solution to the challenges posed by the mucus layer in the nasal cavity [46].

3.4. Determination of Tiagabine

Incorporated TIA amounts of the microneedles were evaluated by HPLC analyses. Analysis results revealed that TIA amounts of the formulations were 5.0% ± 0.1%, 9.8% ± 0.1%, 5.7% ± 0.0%, 10.7% ± 0.0% for C1, C2, E1 and E2, respectively at the day of production (Fig. **8**).

3.5. *In vitro Drug* Release and Release Kinetics

The *in vitro* drug release analyses showed that TIA was released faster from CMC-based microneedles than ES100-based microneedles due to the high water solubility of CMC. The release rates of TIA increased up to 50% after two hours, while release rates reached up to 96.0% and 95.9% for C1 and C2 formulations, respectively, after 24 hours. However, for ES100-based formulations, release rates only reached 10% after two hours, while nearly 88.8% release rates were achieved for both E1 and E2 formulations even at the end of 72 hours (Fig. **9**). The extended release of TIA up to 72 hours with E1 and E2 formulations may enhance the bioavailability of TIA with the nasal application. Analysis results were also evaluated by DDSolver Program to determine the release characteristics of TIA from different types of polymers. TIA releases from CMC-based microneedles fitted to concentration-dependent First-order kinetics due to the aqueous solubility of CMC. On the other hand, ES100-based formulations were fitted to the Hopfenberg kinetic

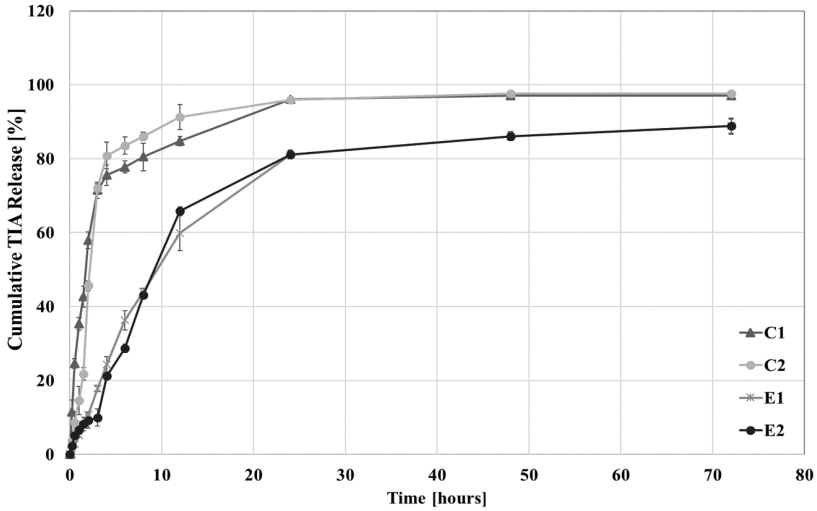


Fig. (9). *In vitro* release analysis results of the microneedles (Mean ± SE; n = 3). *(A higher resolution / colour version of this figure is available in the electronic copy of the article).*

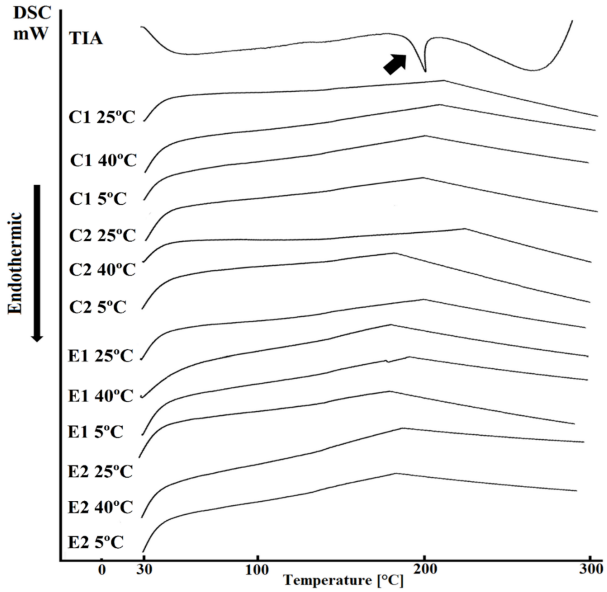


Fig. (10). DSC thermograms of the microneedles at the end of the storage period of six months.

model, which describes drug release from surface-eroding systems with spherical, cylindrical, or planar geometry in accordance with the solubility of ES100 only above pH 7.0 [34, 47, 48].

3.6. Stability Studies

The use of polymeric structure in microneedles has been shown to enhance the stability of incorporated drugs [35]. In stability studies, changes in TIA amounts were evaluated, and analysis results showed that small changes were detected but remained under the limit of 5%, indicating that incorporated TIA remained stable under all storage conditions during the six-month storage period (Fig. **8**) [49]. Possible changes in the structural properties of the microneedles were also evaluated by DSC, FT-IR, and 1H-NMR analyses. DSC analyses were performed at the end of six months to determine temperature-dependent structural changes [50]. DSC analysis results revealed that no endothermic peak related to recrystallization of TIA was revealed in the thermograms of the microneedles indicating that TIA did not exhibit polymorphism and maintained its amorphous state in the formulations under any storage conditions [51]. Microneedles also retained their amorphous structure, demonstrating their structural stability during the storage period (Fig. **10**). FT-IR analyses were performed to determine the structural changes of the polymeric microneedles [42,52]. Differences in the intensities of the characteristic signals of the formulations compared to the initial characterization analyses were detected, most likely due to differences in the amount and batch of the samples (Fig. **11**). ^{1}H-NMR analyses are one of the most important analysis methods for the determination of minor structural

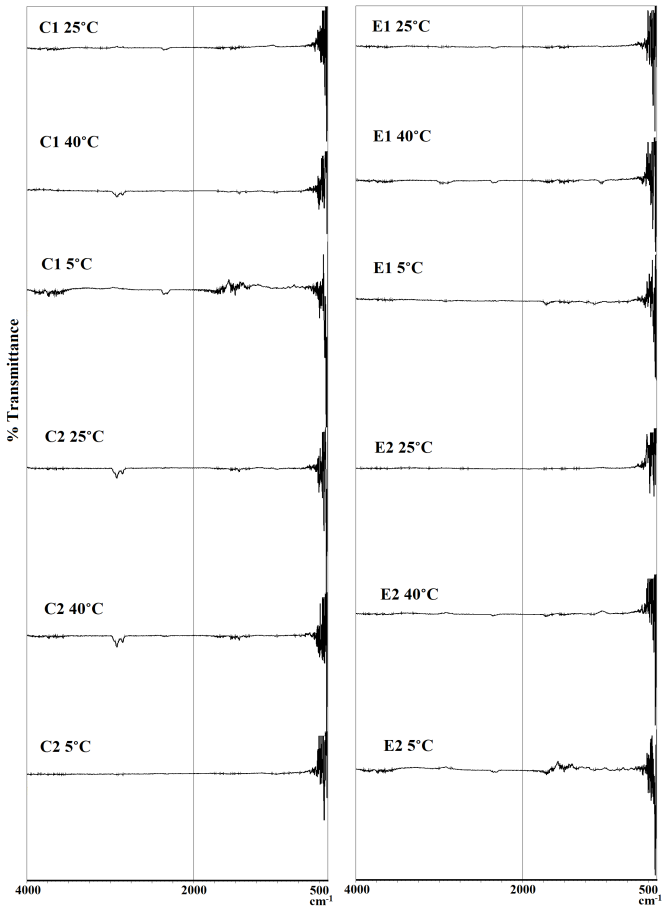


Fig. (11). FT-IR spectra of the microneedles at the end of the storage period of six months.

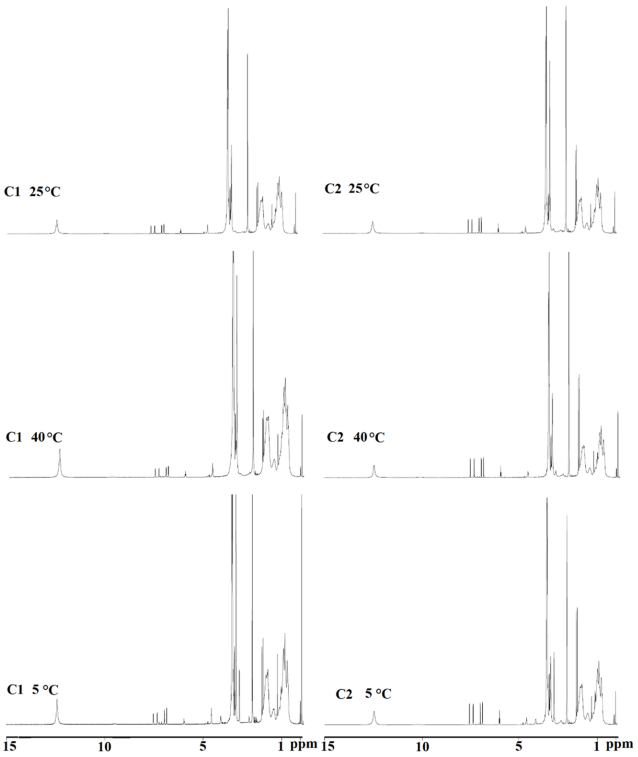


Fig. (12). ^{1}H-NMR spectra of the CMC-based microneedles at the end of the storage period of six months.

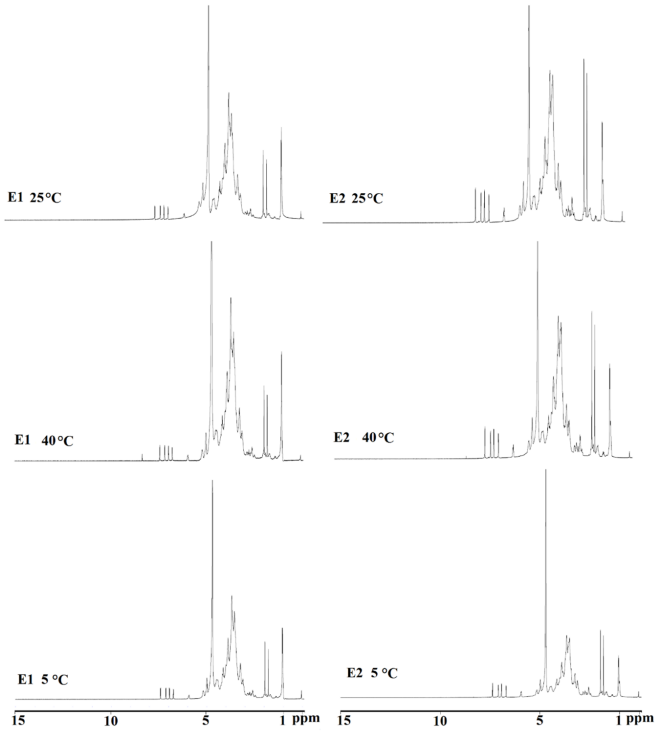


Fig. (13). ^{1}H-NMR spectra of the ES100-based microneedles at the end of the storage period of six months.

changes of the polymeric drug delivery systems [53]. The results of ^{1}H-NMR analyses revealed that, different storage conditions did not affect the characteristic signals of the microneedles during the six-month storage period, indicating the stability of the incorporated drug and the polymeric structure (Figs. **12** and **13**).

CONCLUSION

The significant advantage of the nasal route in epilepsy treatment is direct access to the brain while overcoming the BBB. Therefore, in our study, TIA-loaded microneedles were prepared by micromolding method with CMC and ES100 polymers for possible nasal application. Characterization studies were performed with SEM, DSC, XRD, FT-IR, ^{1}H-NMR, *in vitro* release, and texture analyses. SEM analyses revealed that the incorporation of TIA has influenced the needle morphology, especially for ES100-based microneedles since blunt topped, shorter needles were formed. Depending on the polymer type, sustained releases were achieved up to 72 hours. Microneedles maintained their structural integrity at all storage conditions during the storage period of six months. Considering the high permeability of the nasal epithelium and direct connection to the central nervous system, TIA-loaded microneedles have the potential for the efficient treatment of epilepsy even with the small amounts of TIA while minimizing the side effects through the nasal route. *In vivo* studies will be performed as the next step to strengthen the microneedles' potentials for intranasal application.

LIST OF ABBREVIATIONS

CMC	=	Carboxymethyl Cellulose
DSC	=	Differential Scanning Calorimetry
FT-IR	=	Fourier Transform Infrared Spectroscopy
SEM	=	Scanning Electron Microscopy
TIA	=	Tiagabine Hydrochloride
ES100	=	Eudragit® S 100
XRD	=	X-Ray Diffractometry
^{1}H-NMR	=	Proton Nuclear Magnetic Resonance

ETHICS APPROVAL AND CONSENT TO PARTICIPATE

Not applicable.

HUMAN AND ANIMAL RIGHTS

No humans or animals were used for the studies that are the basis of this research.

CONSENT FOR PUBLICATION

Not applicable.

AVAILABILITY OF DATA AND MATERIALS

The data and supportive information are available within the article.

FUNDING

This study was financed by Anadolu University Scientific Research Project Foundation [Project No: 1901S005].

CONFLICT OF INTEREST

The authors declare no conflict of interest, financial or otherwise.

ACKNOWLEDGEMENTS

The authors would like to acknowledge Anadolu University, Plant, Medicine and Scientific Research Application and Research Center (AUBIBAM) for SEM Analyses, Anadolu University, Faculty of Pharmacy, Central Research Laboratory (MER-LAB) for FT-IR and ^{1}H-NMR Analyses and Eskisehir Technical University, Faculty of Engineering, Department of Materials Science and Engineering for XRD analyses.

REFERENCES

[1] Quintana M, Fonseca E, Sánchez-López J, *et al.* The economic burden of newly diagnosed epilepsy in Spain. Epilepsy Behav 2021; 125(108395): 108395. http://dx.doi.org/10.1016/j.yebeh.2021.108395 PMID: 34781064

[2] Kalser J, Cross JH. New epilepsy treatment in children: Upcoming strategies and rewind to ancient times and concepts. Paediatr Child Health 2018; 28(10): 474-9. http://dx.doi.org/10.1016/j.paed.2018.07.008

[3] Zybina A, Anshakova A, Malinovskaya J, *et al.* Nanoparticle-based delivery of carbamazepine: A promising approach for the treatment of refractory epilepsy. Int J Pharm 2018; 547(1-2): 10-23. http://dx.doi.org/10.1016/j.ijpharm.2018.05.023 PMID: 29751140

[4] Cutillo G, Tolba H, Hirsch LJ. Anti-seizure medications and efficacy against focal to bilateral tonic-clonic seizures: A systematic review with relevance for SUDEP prevention. Epilepsy Behav 2021; 117(107815): 107815. http://dx.doi.org/10.1016/j.yebeh.2021.107815 PMID: 33640562

[5] Antimisiaris SG, Marazioti A, Kannavou M, *et al.* Overcoming barriers by local drug delivery with liposomes. Adv Drug Deliv Rev 2021; 174: 53-86. http://dx.doi.org/10.1016/j.addr.2021.01.019 PMID: 33539852

[6] Yasir M, Sara UVS. Solid lipid nanoparticles for nose to brain delivery of haloperidol: *In vitro* drug release and pharmacokinetics evaluation. Acta Pharm Sin B 2014; 4(6): 454-63. http://dx.doi.org/10.1016/j.apsb.2014.10.005 PMID: 26579417

[7] Khan AR, Liu M, Khan MW, Zhai G. Progress in brain targeting drug delivery system by nasal route. J Control Release 2017; 268: 364-89. http://dx.doi.org/10.1016/j.jconrel.2017.09.001 PMID: 28887135

[8] Matarazzo AP, Elisei LMS, Carvalho FC, *et al.* Mucoadhesive nanostructured lipid carriers as a cannabidiol nasal delivery system for the treatment of neuropathic pain. Eur J Pharm Sci 2021; 159(105698): 105698. http://dx.doi.org/10.1016/j.ejps.2020.105698 PMID: 33406408

[9] Bruinsmann F, Pigana S, Aguirre T, *et al.* Chitosan-coated nanoparticles: Effect of chitosan molecular weight on nasal transmucosal delivery. Pharmaceutics 2019; 11(2): 86. http://dx.doi.org/10.3390/pharmaceutics11020086 PMID: 30781722

[10] Zafar A, Afzal M, Quazi AM, *et al.* Chitosan-ethyl cellulose microspheres of domperidone for nasal delivery: Preparation, in-vitro characterization, in-vivo study for pharmacokinetic evaluation and bioavailability enhancement. J Drug Deliv Sci Technol 2021; 63(102471): 102471. http://dx.doi.org/10.1016/j.jddst.2021.102471

[11] Luppi B, Bigucci F, Cerchiara T, Zecchi V. Chitosan-based hydrogels for nasal drug delivery: From inserts to nanoparticles. Expert Opinion on Drug Delivery. Informa Healthcare 2010; Vol. 7: pp. 811-28. http://dx.doi.org/10.1517/17425247.2010.495981

[12] García-González CA, Sosnik A, Kalmár J, *et al.* Aerogels in drug delivery: From design to application. J Control Release 2021; 332: 40-63. http://dx.doi.org/10.1016/j.jconrel.2021.02.012 PMID: 33600880

[13] Sun M, Yu X, Wang T, Bi S, Liu Y, Chen X. Nasal adaptive chitosan-based nano-vehicles for anti-allergic drug delivery. Int J Biol Macromol 2019; 135: 1182-92. http://dx.doi.org/10.1016/j.ijbiomac.2019.05.188 PMID: 31154036

[14] Tiozzo Fasiolo L, Manniello MD, Tratta E, *et al.* Opportunity and challenges of nasal powders: Drug formulation and delivery. Eur J Pharm Sci 2018; 113: 2-17. http://dx.doi.org/10.1016/j.ejps.2017.09.027 PMID: 28942007

[15] Sonje AG, Mahajan HS. Nasal inserts containing ondansetron hydrochloride based on Chitosan–gellan gum polyelectrolyte complex: *In vitro–in vivo* studies. Mater Sci Eng C 2016; 64: 329-35. http://dx.doi.org/10.1016/j.msec.2016.03.091 PMID: 27127060

[16] Kim JH, Shin JU, Kim SH, *et al.* Successful transdermal allergen delivery and allergen-specific immunotherapy using biodegradable microneedle patches. Biomaterials 2018; 150: 38-48. http://dx.doi.org/10.1016/j.biomaterials.2017.10.013 PMID: 29032329

[17] Sanjay ST, Zhou W, Dou M, *et al.* Recent advances of controlled drug delivery using microfluidic platforms. Adv Drug Deliv Rev 2018; 128: 3-28. http://dx.doi.org/10.1016/j.addr.2017.09.013 PMID: 28919029

[18] Arya J, Henry S, Kalluri H, McAllister DV, Pewin WP, Prausnitz MR. Tolerability, usability and acceptability of dissolving microneedle patch administration in human subjects. Biomaterials 2017; 128: 1-7. http://dx.doi.org/10.1016/j.biomaterials.2017.02.040 PMID: 28285193

[19] Mogusala NR, Devadasu VR, Venisetty RK. Fabrication of microneedle molds and polymer based biodegradable microneedle patches: A novel method. American Journal of Drug Delivery and Therapeutics 2015; 2(2): 60-71.

[20] Andersen TE, Andersen AJ, Petersen RS, Nielsen LH, Keller SS. Drug loaded biodegradable polymer microneedles fabricated by hot embossing. Microelectron Eng 2018; 195: 57-61. http://dx.doi.org/10.1016/j.mee.2018.03.024

[21] Wang M, Hu L, Xu C. Recent advances in the design of polymeric microneedles for transdermal drug delivery and biosensing. Lab Chip 2017; 17(8): 1373-87. http://dx.doi.org/10.1039/C7LC00016B PMID: 28352876

[22] Nguyen HX, Bozorg BD, Kim Y, *et al.* Poly (vinyl alcohol) microneedles: Fabrication, characterization, and application for transdermal drug delivery of doxorubicin. Eur J Pharm Biopharm 2018; 129: 88-103. http://dx.doi.org/10.1016/j.ejpb.2018.05.017 PMID: 29800617

[23] Lee K, Goudie MJ, Tebon P, *et al.* Non-transdermal microneedles for advanced drug delivery. Adv Drug Deliv Rev 2020; 165-166: 41-59. http://dx.doi.org/10.1016/j.addr.2019.11.010 PMID: 31837356

[24] Suriyaamporn P, Opanasopit P, Ngawhirunpat T, Rangsimawong W. Computer-aided rational design for optimally Gantrez® S-97 and hyaluronic acid-based dissolving microneedles as a potential ocular delivery system. J Drug Deliv Sci Technol 2021; 61(102319): 102319. http://dx.doi.org/10.1016/j.jddst.2020.102319

[25] SV H, Darji V, Patel J, Patel B. Stability Indicating Rp-Hplc Method Development and Validation for Estimation of. 2018; 05(04): 2836-61.

[26] Vossler DG, Morris GL III, Harden CL, *et al.* Tiagabine in clinical practice: Effects on seizure control and behavior. Epilepsy Behav 2013; 28(2): 211-6. http://dx.doi.org/10.1016/j.yebeh.2013.05.006 PMID: 23770680

[27] Davies JA. Tiagabine. xPharm: The Comprehensive Pharmacology Reference 2007; 1-4. Available from: https://doi.org/ https://doi.org/10.1016/B978-008055232-3.62759-X

[28] Sills GJ, Rogawski MA. Mechanisms of action of currently used antiseizure drugs. Neuropharmacology 2020; 168(107966): 107966. http://dx.doi.org/10.1016/j.neuropharm.2020.107966 PMID: 32120063

[29] Patil S, Asema SUK, Mirza S. Method development and validation for quantitative analysis of tigabine HCl by ultraviolet spectrophotometry. Int J Chem Sci 2008; 6(1): 413-6.

[30] Lunn G. HPLC methods for recently approved pharmaceuticals. New Jersey, USA: John Wiley and Sons 2005; pp. 1-738. http://dx.doi.org/10.1002/0471711683

[31] ICH Q2 R1 I. ICH Topic Q 2 (R1) Validation of Analytical Procedures: Text and Methodology. 2020. Available from: https://database.ich.org/sites/default/files/Q2%28R1%29%20Guideline.pdf

[32] Choi IJ, Kang A, Ahn MH, *et al.* Insertion-responsive microneedles for rapid intradermal delivery of canine influenza vaccine. J Control Release 2018; 286: 460-6. http://dx.doi.org/10.1016/j.jconrel.2018.08.017 PMID: 30102940

[33] Panda A, Shettar A, Sharma PK, Repka MA, Murthy SN. Development of lysozyme loaded microneedles for dermal applications. Int J Pharm 2021; 593(120104): 120104. http://dx.doi.org/10.1016/j.ijpharm.2020.120104 PMID: 33278495

[34] Zhang Y, Huo M, Zhou J, *et al.* DDSolver: An add-in program for modeling and comparison of drug dissolution profiles. AAPS J 2010; 12(3): 263-71. http://dx.doi.org/10.1208/s12248-010-9185-1 PMID: 20373062

[35] Mönkäre J, Pontier M, van Kampen EEM, *et al.* Development of PLGA nanoparticle loaded dissolving microneedles and comparison with hollow microneedles in intradermal vaccine delivery. Eur J Pharm Biopharm 2018; 129: 111-21. http://dx.doi.org/10.1016/j.ejpb.2018.05.031 PMID: 29803720

[36] Vilar G, Tulla-Puche J, Albericio F. Polymers and drug delivery systems. Curr Drug Deliv 2012; 9(4): 367-94. http://dx.doi.org/10.2174/156720112801323053 PMID: 22640038

[37] Başaran E, Aykaç K, Yenilmez E, Büyükköroğlu G, Tunali Y, Demirel M. Formulation and characterization studies of inclusion complexes of voriconazole for possible ocular application. Pharm Dev Technol 2022; 27(2): 228-41. http://dx.doi.org/10.1080/10837450.2022.2037635 PMID: 35107405

[38] Sanandiya ND, Siddhanta AK. Cellulose-based spreadable new thixo gels: Synthesis and their characterization. RSC Advances 2016; 6(95): 92953-61. http://dx.doi.org/10.1039/C6RA19264E

[39] El-Sakhawy M, Kamel S, Salama A, Hebat-Allah S T. Preparation and infrared study of cellulose based amphiphilic materials. Cellulose chemistry and technology 2018; 52(3–4): 193-200.

[40] Thakral NK, Ray AR, Majumdar DK. Eudragit S-100 entrapped chitosan microspheres of valdecoxib for colon cancer. J Mater Sci Mater Med 2010; 21(9): 2691-9. http://dx.doi.org/10.1007/s10856-010-4109-2 PMID: 20535630

[41] Mourdikoudis S, Pallares RM, Thanh NTK. Characterization techniques for nanoparticles: Comparison and complementarity upon studying nanoparticle properties. Nanoscale 2018; 10(27): 12871-934. http://dx.doi.org/10.1039/C8NR02278J PMID: 29926865

[42] Sughir A, Skiba M, Lameiras P, Coadou G, Lahiani-Skiba M, Oulyadi H. Study of interaction between tiagabine HCl and 2-HPβCD: Investigation of inclusion process. J Incl Phenom Macrocycl Chem 2010; 68(1-2): 55-63. http://dx.doi.org/10.1007/s10847-009-9732-5

[43] Pawar P, Sharma P, Chawla A, Mehta R. Formulation and *in vitro* evaluation of Eudragit S-100 coated naproxen matrix tablets for colon-targeted drug delivery system. J Adv Pharm Technol Res 2013; 4(1): 31-41. http://dx.doi.org/10.4103/2231-4040.107498 PMID: 23662280

[44] Zhao X, Li X, Zhang P, Du J, Wang Y. Tip-loaded fast-dissolving microneedle patches for photodynamic therapy of subcutaneous tumor. J Control Release 2018; 286: 201-9. http://dx.doi.org/10.1016/j.jconrel.2018.07.038 PMID: 30056119

[45] Beule AG. Physiology and pathophysiology of respiratory mucosa of the nose and the paranasal sinuses. GMS Curr Top Otorhinolaryngol Head Neck Surg 2010; 9: Doc07. http://dx.doi.org/10.3205/cto000071 PMID: 22073111

[46] Khosa A, Reddi S, Saha RN. Nanostructured lipid carriers for site-specific drug delivery. Biomed Pharmacother 2018; 103: 598-613. http://dx.doi.org/10.1016/j.biopha.2018.04.055 PMID: 29677547

[47] Franco P, De Marco I. Eudragit: A novel carrier for controlled drug delivery in supercritical antisolvent coprecipitation. Polymers 2020; 12(1): 234. http://dx.doi.org/10.3390/polym12010234 PMID: 31963638

[48] Sivasankaran S, Jonnalagadda S. Advances in controlled release hormonal technologies for contraception: A review of existing devices, underlying mechanisms, and future directions. J Control Release 2021; 330: 797-811. http://dx.doi.org/10.1016/j.jconrel.2020.12.044 PMID: 33370578

[49] Center for Drug Evaluation and Research. Q2(R1) validation of analytical procedures: text and methodology. 2003. http://dx.doi.org/10.32388/YOKP53

[50] Coban O, Aytac Z, Yildiz ZI, Uyar T. Colon targeted delivery of niclosamide from β-cyclodextrin inclusion complex incorporated electrospun Eudragit® L100 nanofibers. Colloids Surf B Biointerfaces 2021; 197(111391): 111391. http://dx.doi.org/10.1016/j.colsurfb.2020.111391 PMID: 33129100

[51] Zhou B, Liu S, Yin H, Qi M, Hong M, Ren GB. Development of gliclazide ionic liquid and the transdermal patches: An effective and noninvasive sustained release formulation to achieve hypoglycemic effects. Eur J Pharm Sci 2021; 164(105915): 105915. http://dx.doi.org/10.1016/j.ejps.2021.105915 PMID: 34146681

[52] Abilova GK, Kaldybekov DB, Ozhmukhametova EK, *et al.* Chitosan/poly(2-ethyl-2-oxazoline) films for ocular drug delivery: Formulation, miscibility, *in vitro* and *in vivo* studies. Eur Polym J 2019; 116: 311-20. http://dx.doi.org/10.1016/j.eurpolymj.2019.04.016

[53] Singh RB, Das N, Singh GK, Singh SK, Zaman K. Synthesis and pharmacological evaluation of 3-[5-(aryl-[1,3,4]oxadiazole-2-yl]-piperidine derivatives as anticonvulsant and antidepressant agents. Arab J Chem 2020; 13(5): 5299-311. http://dx.doi.org/10.1016/j.arabjc.2020.03.009

DISCLAIMER: The above article has been published, as is, ahead-of-print, to provide early visibility but is not the final version. Major publication processes like copyediting, proofing, typesetting and further review are still to be done and may lead to changes in the final published version, if it is eventually published. All legal disclaimers that apply to the final published article also apply to this ahead-of-print version.